

Energy Dependence of the Fragmentation of UH-Nuclei

L. Y. Geer⁽¹⁾, J. Klarmann⁽¹⁾, B. S. Nilsen⁽²⁾, C.J. Waddington⁽²⁾,
 W. R. Binns⁽¹⁾, J. R. Cummings⁽³⁾, and T. L. Garrard⁽³⁾
 (1)Washington University, (2)University of Minnesota, (3)Caltech

ABSTRACT

The fragmentation of 10.6 GeV/n Au in CH₂, C, Al, Cu, Sn, and Pb targets has been studied using an array of ion chambers, multi-wire proportional counters (MWPC), and Cherenkov counters. Total charge-changing cross sections were found to be monotonically increasing with target charge over cross sections measured and derived from lower energy data. Partial charge-changing cross sections yielding charge changes less than 10 were depressed from those measured at lower energy.

1. INTRODUCTION

Nuclear cross sections are needed to model the propagation of UH-nuclei ($Z \geq 30$) through the interstellar medium and to account for the interactions in detectors. Our earlier experiments^{1,2,3} to determine the cross sections of heavy UH-nuclei were constrained by the maximum energy of the LBL Bevalac, which limited gold projectiles to $\lesssim 1$ GeV/n. These energies are significantly below the average energies of the UH-nuclei observed in the cosmic radiation. Furthermore, many of the important cross sections were found to be still varying at the highest energies available. In April 1992 the BNL AGS produced the first beam of gold nuclei with an energy of 10.6 GeV/n or 2.1 TeV per nucleus. Here we will report preliminary results from a study of interactions at this energy.

2. EXPERIMENT

Figure 1 shows the layout of the detectors for AGS experiment 869, similar to the arrays used in our previous experiments.^{1,2,3} The layout can be divided into several sections. The beam definition section allowed the selection of a beam containing only Au nuclei with a limited spatial distribution. Each target, CH₂, C, Al, Cu, Sn, and Pb, was ~ 0.2 interaction lengths thick. A target-out run was obtained and used to correct for interactions in the detectors. Hydrogen cross sections were derived by subtraction of the C cross sections from the CH₂ cross sections.

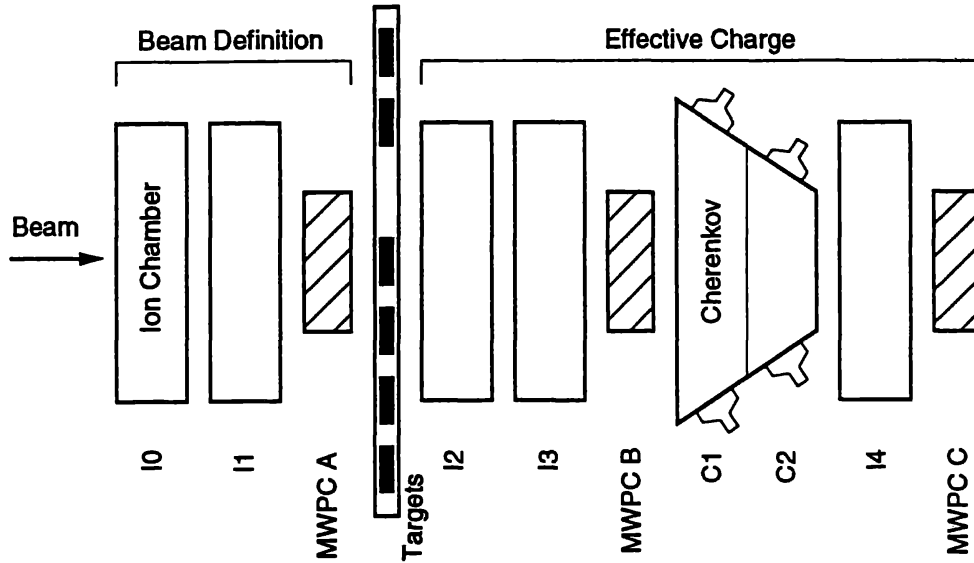
After passing through the target area, the effective charge

$$Z' = \sqrt{\sum_{i=1}^n Z_i^2} \quad (1)$$

was determined for the n particles exiting the target and passing through the array.

Preliminary examination of the accelerator data revealed excellent charge resolution, better than 0.15 charge units in the Cherenkov detectors and 0.28 charge units in the sum of two ion chambers. This resolution is shown in Figure 2.

Figure 1: Layout of the detector array.



3. ANALYSIS AND RESULTS

3.1 Total Cross Sections

The incident gold beam was defined by requiring the ionization signal to be within $\pm 1.5\sigma$ of the beam peak in detectors I0 and I1, where σ is the standard deviation of a gaussian fit to the beam peak. The position of the beam was selected to be within $\pm 2\sigma$ of the peak signal in both the x and y directions of MWPC A, where the distribution was gaussian with $\sigma \sim 0.75$ cm.

Total charge-changing cross sections were measured by counting the number of non-interacting particles in the target-in run and using the target-out run to count the number of particles that interacted in material other than the target. The number of gold nuclei counted in the Cherenkov detectors is

$$N = N_0 \exp(-x_d/\lambda_d) \exp(-x_i/\lambda_i) k_1 k_2, \quad (2)$$

where N_0 is the number of incident beam particles as defined above; x_d is the thickness and λ_d is the mean free path in g/cm^2 of the material between the target and C1; and x_i and λ_i are the thickness and mean free path of the target. The constant k_1 represents particles that interacted in the Cherenkov detectors but were counted as gold nuclei because their effective charge was sufficiently close to 79. The correction factor k_2 accounts for gold nuclei in the tails of the gold peak not included in the selection. A similar expression to (2) exists for the target out run:

$$N' = N'_0 \exp(-x_d/\lambda_d) k_1 k_2, \quad (3)$$

where N' is the number of Au in the Cherenkov and N'_0 is the number in the incident beam. Dividing (2) by (3) we obtain

$$\lambda_i = x_i \left(\ln \frac{N_0 N'}{N'_0 N} \right)^{-1}, \quad (4)$$

and then

$$\sigma_T = \frac{\langle A \rangle}{\lambda_i} \cdot 6.022 \times 10^4, \quad (5)$$

where σ_T is the total cross section in mb, $\langle A \rangle$ is the average atomic number of the target, and λ_i is in g/cm^2 .

Since the mean and standard deviation of the gold peak varied from target to target, it was necessary that k_1 and k_2 be kept constant for the target-in and target-

out run. To accomplish this, we defined a set of nuclei that can be identified as gold passing through the entire telescope by making a $\pm 1\sigma$ selection on the beam peak in I4. Using this set, C1+C2 was histogrammed and fit with a gaussian. The mean and σ of this fit was used to define a $\pm 2.5\sigma$ selection on C1+C2. After removing the selection on I4, this selection was performed on the run data to determine N . Varying the selection from 2.0 to 2.75 σ did not change the cross sections by an amount greater than statistical error. The charge-changing cross sections and statistical errors are listed in Table 1 and compared in Figure 3 to previous measurements made with 1.0 GeV/n Au and to a modified hard sphere relation described earlier.¹ The differences between the cross sections measured at 10.6 GeV/n and those measured and derived at the lower energy increase monotonically with target charge. The difference is insignificant for H.

TABLE 1: Total Cross sections in mb

Target	H	CH ₂	C	Al	Cu	Sn	Pb
σ_T	1475 \pm 53	1919 \pm 31	2808 \pm 51	3470 \pm 67	4361 \pm 80	5375 \pm 103	6576 \pm 108
σ_T^1	1426 \pm 65	1861 \pm 63	2731 \pm 58	3240 \pm 82	-	-	-

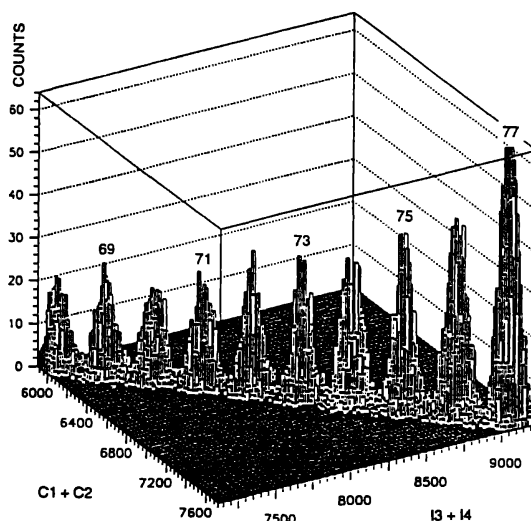


Figure 2: Two dimensional histogram of Cherenkov signals v. ion chamber signals. Numbers at the top of the peaks are the charges of the peaks.

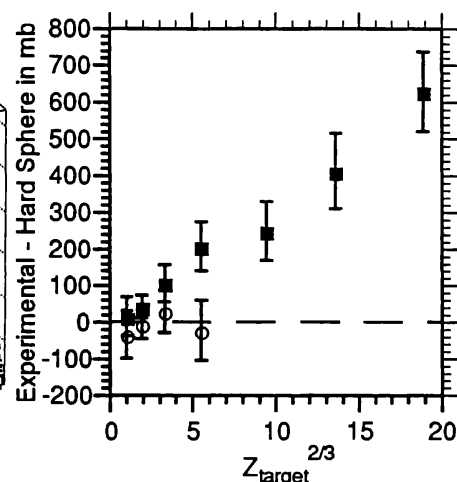


Figure 3: Deviations of total cross sections from a modified hard sphere relation¹ as a function of $Z_{\text{target}}^{2/3}$. Squares are data from this paper; Circles are experimental values from Binns *et al.*¹

3.2 Partial Cross Sections

Partial cross sections were determined using the same beam definition selections as in the total cross section analysis. To count the secondaries produced, several corrections were applied to the data.

Because of their charge resolution, the Cherenkov detectors were used to measure the charges of the secondaries. Since the Cherenkov detectors have an appreciable thickness (~ 0.3 interaction lengths), it was necessary to eliminate interacting nuclei with a consistency selection. This selection was achieved by histogramming I4-I3 for several different charge regions and fitting a gaussian to the largest peak, which contained nuclei that did not interact between I3 and I4. The means and standard deviations of these fits were used to define a $\pm 2\sigma$ consistency selection in I4-I3. After applying this selection it was necessary to add back the

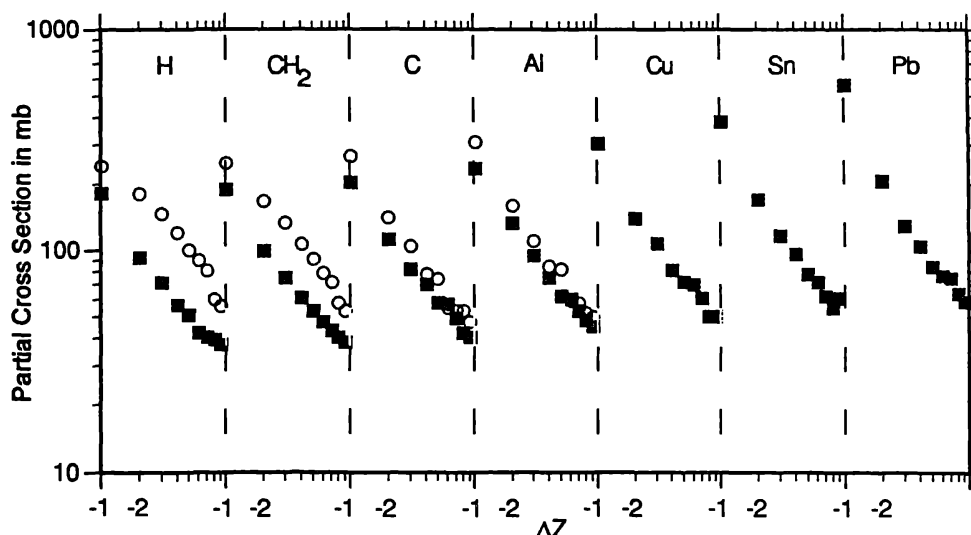
number of secondaries eliminated. This was done by using the expression for total cross section derived at lower energies by Binns *et al.*¹ scaled to the total cross section data described in this paper.

A second correction to the data was necessary to compensate for nuclei that interacted in the non-target matter between the Cherenkov detectors and the charge definition section of the detector. This correction was accomplished by subtracting the histogram of C1+C2 of a target-out run from a target-in run, normalizing the counts in the target-out run to have the same number of gold nuclei in the Cherenkov detectors as the target-in run.

Since the target has a finite thickness, it is possible that nuclei could make multiple interactions in the target. Therefore, a thick target correction was made as described in Cummings *et al.*²

Taking into account all of these corrections, the partial cross sections found are graphed in Figure 4. Comparison to previous experiments^{1,2} shows a decrease in partial cross sections, particularly for small changes in charge and light targets. In particular for H, the constancy of σ_T suggests that the partial cross sections for large charge change must be appreciably greater than those at low energy.

Figure 4: Partial cross sections for $\Delta Z = -1$ to -9 . Squares are data from this paper; Circles are 1.0 GeV/n data from Binns *et al.*¹



Acknowledgements: This work was supported in part by NASA and DOE. We thank E. C. Stone, B.W. Gauld, Dana Beavis, and the staff of Brookhaven National Laboratory.

REFERENCES

1. W. R. Binns *et al.*: 1987, Phys. Rev. C, 36, 1870.
2. J. R. Cummings *et al.*: 1990, Phys. Rev. C, 42, 2508 and 2530.
3. B. S. Nilsen *et al.*: 1993, This conference, session OG.